

The mean hydration of carbohydrates as studied by normalized two-dimensional radial pair distributions

Claus Andersson and Søren Balling Engelsen

Food Technology, Department of Dairy and Food Science, The Royal Veterinary and Agricultural University, Frederiksberg, Denmark

The hydration of carbohydrates plays a key role in many biological processes. Molecular dynamics simulations provide an effective tool for investigating the hydration of complex solutes such as carbohydrates. In this article we devise an algorithm for the calculation of two-dimensional radial pair distributions describing the probability of finding a water molecule in a site defined by two reference atoms. The normalized 2D radial pair distribution is proposed as an effective tool for investigating and comparing localized or ordered water sites around flexible molecules such as carbohydrates when analyzing molecular dynamics simulations and the utility of 2D radial pair distributions is demonstrated using sucrose as an example. In this relatively simple structure, 2D radial pair distributions were able to characterize and quantify the importance of two unique interresidue hydration sites in which a water molecule is forming a bridge between the glycopyranosyl and fructofuranosyl residues. The approach is proposed to be a valuable tool for comparing and understanding the hydration of flexible biomolecules such as carbohydrates. © 2000 by Elsevier Science Inc.

Keywords: pair distributions, hydration, molecular dynamics, sucrose

INTRODUCTION

The next frontier in the understanding of carbohydrate structure and functionality will most likely be focused around their hydration. In foods carbohydrates provide energy, sweet taste, and structure, and in all three aspects water is believed to play

a decisive role. However, at the molecular level it is not known to what extent water contributes to energy metabolism and sweet taste perception as a structural element in addition to its carrier function. In carbohydrate-based gels, which are abundantly used in food products because of their excellent mouthfeel, chewing and flavor release properties, it is not known in detail how water functions as a structural element. In solid systems carbohydrates tend to cocrystallize with water and water is an important brick in building the structure of the starch granule.¹ To obtain a better understanding of the dynamic and static interactions between carbohydrates and water, one feasible route is to perform molecular dynamics simulations with explicitly present water molecules.

Molecular dynamics (and Monte Carlo) simulations of solutes in water provide a unique possibility for detailed examination of water–solute interactions. However, when such simulations are performed, the question arises: “How does one characterize water solvating a complex solute?”² The large number of water molecules, the complexity of the solute, and the high degree of mobility in such simulations require a statistical approach to describe the hydration. Radial pair distributions, orientational pair distribution, and static water densities with the solute as reference are the most commonly statistical approaches employed to examine water–water and water–solute interactions.

Radial pair distributions have the longest history and an experimental background. In a pure water system the radial oxygen–oxygen pair distribution functions, $g(r_{\text{Ow}}, r_{\text{Ow}})$, can be measured from X-ray scattering experiments, assuming that the X-ray intensities are dominated by spherical scattering centered at the oxygens.³ Radial pair distributions of specific solute nuclei and the oxygen nuclei in water have been used in the literature to describe the large differences in the first and second hydration shells of different types of atoms, e.g., around carbon in methyl and methylene groups, which have a typical hydrophobic behavior, and around oxygen in hydroxyl groups, which have a typical hydrophilic behavior.⁴ Radial pair distributions have also been used to scrutinize the detailed hydration pattern around solute atoms.^{5–7} However, because of compli-

Color Plates for this article are on pages 131–133.

Corresponding author: Dr. Søren Balling Engelsen, Food Technology, Department of Dairy and Food Science, The Royal Veterinary and Agricultural University, Rolighedsvej 30, DK-1958 Frederiksberg C, Denmark. Tel.: +45 35 28 32 05; fax: +45 35 28 32 45.

E-mail address: se@kv1.dk (Søren Balling Engelsen)

cated dynamic and steric effects, such efforts are in general not convincing. While radial pair distributions are useful in analyzing the hydration density around specific atoms, in general they carry only hidden information on localized hydration sites. This information may in principle be improved by using orientational distribution functions,⁸ which are usually applied to characterize the orientational preferences of local (first hydration shell) water molecules around solute atoms ($X \cdots H-Ow$). It can also be used to examine the orientational preferences of water density with respect to a given solute vector $X-X \cdots Ow$.⁷

A much clearer picture of the solute hydration is obtained by calculating and contouring 3D water densities in a fixed frame defined by the solute.^{2,9} However, this approach has two major disadvantages, namely the difficulties in visualizing the densities in three dimensions and that it is useful only for rigid molecules or rigid molecular segments.

While the hydration around monosaccharides and other relatively rigid molecules can be well described by static water densities or radial pair distributions with only one reference point, the introduction of the glycosidic linkage principle in carbohydrates introduces such a high degree of flexibility that another approach for describing the hydration pattern is needed. Normalized 2D radial pair distribution is one such tool for describing hydration sites around highly flexible carbohydrates. Two-dimensional radial pair distribution, which to our knowledge was first introduced in a nonnormalized application by Immel and Lichtenthaler,¹⁰ does not suffer from the above-mentioned disadvantages, as these can be contoured in two dimensions and they take into account the complex dynamics of the solute.

In this investigation normalized 2D pair distribution is applied for the analysis of a molecular dynamics simulation of sucrose (β -D-fructofuranosyl-(2 \rightarrow 1)- α -D-glucopyranoside) in a diluted aqueous solution. However, the algorithm devised is not restricted to carbohydrates and may prove to be useful in studies of protein hydration and in studies of interfacial behavior between liquids and solids.

TWO-DIMENSIONAL PAIR DISTRIBUTIONS

The radial pair distribution function $g(r)$ gives the probability of finding a pair of atoms a distance r apart, relative to the probability expected for a random distribution at the same density.

$$g(r) = \frac{N(r)}{\rho_w \times \frac{4}{3} \pi \times [(r + \Delta r)^3 - r^3]} \quad (1)$$

where ρ_w is the water density. It is evaluated by calculating the distance, r , between the pair of atoms and then adding it to a histogram divided into a number of Δr subintervals. The probability of finding the atom pair in the sphere shell defined by the radii r and $r + \Delta r$ is related to the volume.

The 2D radial pair distribution function $g(r_1, r_2)$ gives the probability of finding an atom (e.g., water oxygen) at a distance r_1 and r_2 from two selected solute atoms, relative to the probability expected for a random distribution.

$$g(r_1, r_2) = \frac{N(r_1, r_2)}{\rho_w \times V_{\text{intersect}}(r_1, r_2, \Delta r)} \quad (2)$$

The calculation of 2D radial pair distributions is analogous to 1D radial pair distribution, except that the histogram is now two dimensional, referring to two reference points (nuclei) instead of one, and the normalization is more complicated. The 2D radial pair distributions must be normalized using the intersection volume of the two sphere shells, $V_{\text{intersect}}$.

Algorithm for Two-Dimensional Normalization

When calculating the intersection volume we consider two atoms, A and B , connected through their centers by a virtual axis, as depicted in Figure 1. The center of atom A defines the *zero* of the axis, and on this axis the distance between the atoms is R . Two spheres circumscribe atom A , the innermost with radius r_A and the outermost with radius R_A . Likewise, two spheres circumscribe atom B , with radii r_B and R_B . For both atoms, a spherical cavity (or shell) is defined by the space between the inner and the outer spheres. The thickness of this cavity is equal for A and B , and is designated $\Delta r = R_A - r_A = R_B - r_B$. The task is to calculate the volume of the intersection of the two spherical cavities, as indicated in Color Plate 1.

The task of calculating the volume of a sphere section (slice), limited by two planes perpendicular to its radius, is a significant subproblem in this regard. Let x_1 define the intersection point of the first limiting plane and let x_2 define the intersection point of the second plane on the axis common to both atoms. Initially, an expression is derived for a sphere circumscribing atom B , which has its center located at R . For atom A , the same solution applies for $R = 0$. Using the nomenclature described above, the solution is as described

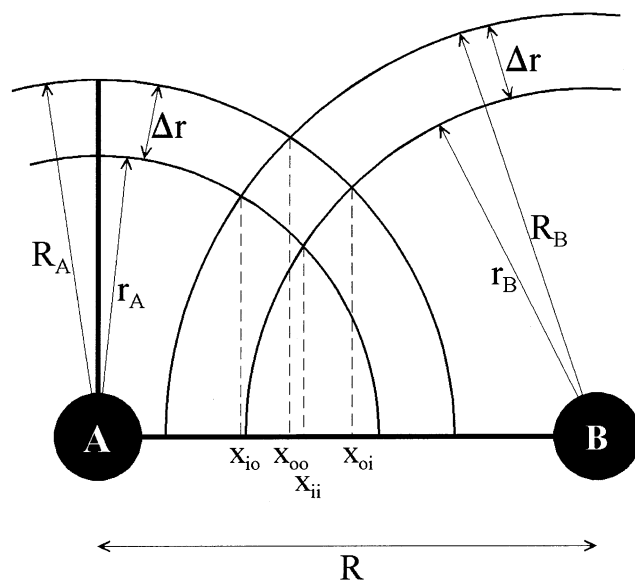


Figure 1. Schematic diagram of hydration shells with indications of relevant parameters for calculating 1D and 2D pair distributions.

in Eq. (3) subject to $(x_1, x_2, r, R \in \mathcal{R} \mid x_1 < x_2 \wedge \{x_1, x_2\} \in [R - r, R + r])$,

$$\begin{aligned} V(x_1, x_2, r, R) &= \pi \int_{x_1}^{x_2} y(x, r, R)^2 dx \\ &= \pi \int_{x_1}^{x_2} r^2 - (x - R)^2 dx \\ &= \frac{\pi}{3} (x_1^3 - x_2^3) + \pi R (x_2^2 - x_1^2) \\ &\quad + \pi (x_2 - x_1)(r^2 - R^2) \quad (3) \end{aligned}$$

Given V , the problem simplifies to identify x_1 and x_2 , since r is either r_A, R_A, r_B , or R_B and R is zero (0) in the case of atom A. In the numerical simulation it holds that $\Delta r \ll r_A$. Using this simplification, seven distinct cases can be identified. Not all are equally important, since some are special cases that rarely occur. To simplify the presentation, we define the following scalars:

$$\begin{aligned} x_{ii} &= \frac{1}{2R} (r_a^2 + R^2 - r_b^2) \\ x_{io} &= \frac{1}{2R} (r_a^2 + R^2 - R_b^2) \\ x_{oi} &= \frac{1}{2R} (R_a^2 + R^2 - r_b^2) \\ x_{oo} &= \frac{1}{2R} (R_a^2 + R^2 - R_b^2) \quad (4) \end{aligned}$$

Using these definitions, we derive the following seven cases:

Case I $(R - r_B \leq -R_A)$ (5)
 $V^I = 0$

Case II $(-R_A < R - r_B \leq -r_A)$
 $V^{II} = V(-r_A, x_{oi}, R_A, 0) - V(R - r_B, x_{oi}, r_B, R)$

Case III $(-r_A < R - r_B \leq R_A)$
 $V^{III} = V(R - R_B, x_{oo}, R_B, R) + V(x_{oo}, x_{oi}, R_A, 0)$
 $- V(-r_A, x_{ii}, r_A, 0) - V(x_{ii}, x_{oi}, r_B, R)$

Case IV $(-r_A < R - R_B < R - r_B \leq r_A)$
 $V^{IV} = V(x_{io}, x_{oo}, R_B, R) + V(x_{oo}, x_{oi}, R_A, 0)$
 $- V(x_{io}, x_{ii}, r_A, 0) - V(x_{ii}, x_{oi}, r_B, R)$

Case V $(r_A < R - r_B < R_A)$
 $V^V = V(x_{io}, x_{oo}, R_B, R) + V(x_{oo}, x_{oi}, R_A, 0)$
 $- V(x_{io}, R_A, r_A, 0) - V(R - r_B, x_{oi}, r_B, R)$

Case VI $(r_A \leq R - R_B < R_A)$
 $V^{VI} = V(R - R_B, x_{oo}, R_B, R) + V(x_{oo}, R_A, R_A, 0)$

Case VII $(R_A \leq R - R_B)$
 $V^{VII} = 0$ (5)

In practice, 2D pair distributions are averaged over an entire molecular dynamics trajectory, for which reason the 2D pair distribution histogram will have to be normalized with the number of trajectory frames included and by the water density in the simulation.

HYDRATION OF SUCROSE AS AN EXAMPLE

The molecular dynamics trajectory analyzed with 2D radial pair distributions in this study was carried out as a microcanonical ensemble over 0.5 ns, containing 1 sucrose molecule (Figure 2) and 489 water molecules and using minimum convention periodic boundary conditions. The simulation was recorded using the CHARMM program,¹¹ applying the modified carbohydrate force field¹² for the solute and the simple three-site TIP3P force field for the water molecules.¹³ The system with a concentration of 3.74% (w/w) was equilibrated at 300 K and complete phase points were saved every 0.02 ps for subsequent analysis (simulation details are given elsewhere^{7,14,15}). In this trajectory the presence of water was found to alter the accessible conformational space of sucrose significantly and to improve the theoretical models. With water explicitly included in the model, internal and overall motions of sucrose were found to compare extremely well with glycosidic heteronuclear coupling constants, NOESY volumes, molecular tumbling time, radius of gyration, and translational diffusion coefficients established from experimental studies.

Before describing the 2D radial pair distributions around hydroxylic solute oxygen atoms it must be emphasized that with the force field applied, the 1D pair distributions of the hydroxylic oxygens display typical hydrophilic hydrogen bonding behavior with a strong radial water structuring. The first hydration shell is characterized by a sharp first peak at 2.8 Å with a density of approximately 2.2 times the bulk density and a first minimum at 3.7 Å with a density of a little more than half the bulk density, indicating the outer limit of the first hydration shell. The radial pair distribution functions of the hydroxylic oxygen also show some long-range structure with a peak at approximately 5.5 Å, indicating the center of the secondary hydration shell.⁷

When implemented, the calculation of 2D radial pair distribution is a relatively quick procedure and with advantage can be calculated simultaneously with 1D radial pair distributions

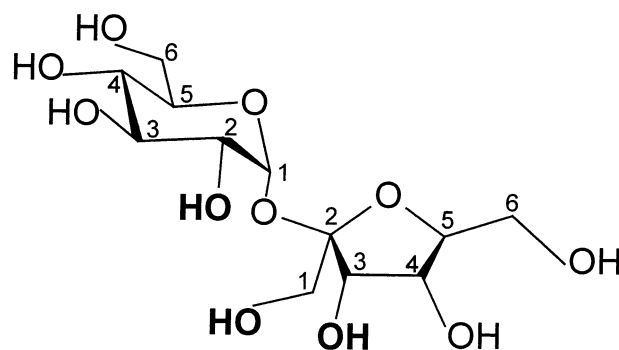


Figure 2. Schematic representation of sucrose. The important hydroxyl groups at positions O-2g, O-1f, and O-3f are marked in boldface.

for screening of the trajectory. In this study we have chosen the four most interesting 2D pair distributions for further discussion. The first result of the 2D radial pair distribution calculations, which we will discuss and use as a reference, is the $g(r_{O2g...Ow}, r_{O3g...Ow})$ 2D pair distribution shown in Color Plate 2a. Color Plate 2a shows the normalized 2D radial pair distribution of water in which the solute atoms O-2g and O-3g are the reference sites and provide information on the magnitude of the shared water density between two neighboring equatorial pyranosyl secondary hydroxyl groups. The maximum shared water density of 5.6 times the bulk density (1.0) is found in the lower left corner (2.8 Å, 2.8 Å) and is a result of an advantageous position of the water in the center of the two solute oxygen's first hydration shell. This shared maximum density of 5.6 is stronger than the average 1D pair distribution peak density (approximately 2.2) of the first hydration shell, indicating a substantial anisotropy of the latter. Other features observed in Color Plate 2a are two *elongated* hydration regions (4.0 to 5.5 Å) along $r_{Ow...O2g} = 2.8$ Å and $r_{Ow...O3g} = 2.8$ Å respectively, with water densities above bulk density (3.5 and 2.8, respectively). These are more complex hydration phenomena, but describe mainly the hydration sites around O-1g and O-4g. Their relatively low density and nonlocalized shape indicates that the O-2g ··· O-3g vector is not a strongly conserved structural motif with respect to the water structure. At longer distances from the two solute oxygens we find less structured water and observe that the shared water density approaches 1.0, corresponding to the bulk density. The rapid decline of shared water densities to zero at approximately 6 Å is simply explained by the fact that it is an impossible situation, as the two sphere shells do not intersect (Case I). In the trajectory the average O-2g ··· O-3g distance (R) was 2.88 Å, ranging from 2.55 to 3.27 Å, allowing also for a direct but geometrically restricted hydrogen bond.

The next example in Color Plate 2b displays the 2D radial pair distribution of water oxygens with O-2g and O-4g as reference points, $g(r_{O2g...Ow}, r_{O4g...Ow})$. In this figure we observe that there is no density build-up due to shared first hydration shell waters. In the trajectory the average O-2g ··· O-4g distance was 4.88 Å, ranging from 4.51 to 5.22 Å, indicating that a geometrical situation with a bridging water is possible. However, apparently such a situation is too sterically and entropically restricted to be of any significance. In contrast to the $g(r_{O2g...Ow}, r_{O3g...Ow})$ distribution in Color Plate 2a we observe that the water density is strongly localized around the two atoms with no directly shared water molecules. The peak maxima found at approximately $R = 5.6$ Å owing to shared water density with O-1g or O-6g are stronger (approximately 4.6 times the bulk density) and less diffuse than the corresponding neighboring peaks in the $g(r_{O2g...Ow}, r_{O3g...Ow})$ distribution. This observation indicates that the O-2g ··· O-4g vector is a highly conserved structural motif with respect to the water structure and is in agreement with the finding that the equatorial/axial configurations at O-2 and O-4 in pyranoses are essential for maintaining the overall compatibility with the three-dimensional hydrogen-bonded network of water.¹⁶

In Color Plates 2c and d, 2D radial pair distributions are displayed as a function of hydroxylic oxygens placed on opposite sucrosyl rings. Color Plate 2d displays the 2D radial pair distribution between O-2g and O-3f, $g(r_{O2g...Ow}, r_{O3f...Ow})$, from which we observe a strong and sharp shared water density with a peak density of approximately 3.5 times bulk water

density. In the case of the O-2g ··· O-3f distance the trajectory average was 5.08 Å, ranging from 4.07 to 6.10 Å, indicating a rather flexible situation for the two reference atoms across the glycosidic linkage. This bridging water density between the O-2g and O-3f hydroxyl groups, first reported by Engelsen et al.,¹⁴ compares well with the crystal structure of two sucrose molecules buried and partially hydrated in the binding site of a lentil-lectin complex.¹⁷ Both of these sucrose structures were observed hydrated with an interresidue bridging water molecule (oxygen) between O-2g and O-3f.

Color Plate 2c displays the 2D radial pair distribution between O-2g and O-1f, $g(r_{O2g...Ow}, r_{O1f...Ow})$, from which we observe an extremely strong and sharp shared water density with a peak maximum of approximately 8.5 times the bulk density. This is an extreme situation, being more populated than a shared water between two neighboring pyranose hydroxyl groups displayed in Color Plate 2a and thus far the best example of a localized or "pocket" water molecule we have been able to detect in a condensed phase molecular dynamics simulation of small carbohydrates. The trajectory average of the O-2g ··· O-1f distance was 4.04 Å, ranging from 2.48 to 6.32 Å, and by this criterion the most flexible frame of reference investigated in this study (maximum distance difference of 3.84 Å). For this reason the contour plot in Color Plate 2c reveals only weak secondary features. This water molecule bridging the two sugar rings has previously been detected independently by Immel and Lichenthaler¹⁰ and Engelsen and Pérez⁷ by performing molecular dynamics in two quite different carbohydrate/water force fields, GROMOS and CHARMM.¹⁸ It was reported to be populated ($R_A, R_B \leq 3.5$ Å) two-thirds of the trajectory time,⁷ but with the normalized 2D radial pair distribution we now have a tool to quantify the magnitude of the localized water density and compare it with other sites and other molecular dynamics simulations.

Color Plate 3 shows the trajectory of the most resident water molecule in an oblong cavity defined by O-2g on one side and O-1f and O-3f on the other side. From Color Plate 3 it is observed that the water molecule stays for almost 80 ps in the cavity defined by the three oxygen atoms O-2g, O-1f, and O-3f. We have previously calculated that the maximum residence time a bridging water (oxygen) stays in the first hydration shell around both O-2g and O-3f and around O-2g and O-1f was approximately 9 ps⁷ in both cases, which illustrates the concerted action of this hydration site. In this example the water enters the cavity in a complex trajectory starting by a "capture" via the O-3f group. The expulsion of the water from the other side of the cavity is more rapid. Given the high probability of finding a bridging water in this cavity and the good agreement with experimental entities provided by the simulation,^{7,14} it is tempting to propose that this hydration characteristic is of prime importance to the sucrose crystallization process, sucrose supersaturation behavior, sucrose transport in plants, and sweet taste reception including the transport of the sucrose into the receptor epithelium, all of which are processes that occur in aqueous environments.

CONCLUSIONS

An algorithm has been provided to normalize 2D pair distribution functions. Two-dimensional radial pair distributions have been used to examine the hydration behavior in a condensed phase molecular dynamics simulation, using sucrose as

an example. In the example we observe a carbohydrate(–water) structure that would not have been detected without explicit waters present in the simulation and that would not easily have been detected and quantified without the use of 2D pair distributions. The maximum shared water density of 8.5 times the bulk density calculated for the O-2g · · Ow · · O-1f situation is to date the most extreme/resident example of a bridging water and significantly influences the solvated carbohydrate structure. This bridging water is proposed to have implications for both physical and biological sucrose activities. Future research in the hydration of related saccharides and polysaccharides will reveal if this strong and specific hydration of sucrose is unique or if alternative hydration patterns across the glycosidic linkages exist, and 2D radial pair distributions will be an ideal platform for comparing hydration sites across solute structures and simulations.

ACKNOWLEDGMENTS

C.A. was supported by the Center for Predictive Multivariate Process Analysis, financed by the Danish Governmental Department for Industry and by the Research Councils; and S.B.E. was supported by the Centre of Advanced Food Studies (LMC) in a project concerning molecular modeling of carbohydrates. We thank Professor Lars Munck for supporting this work and Gilda Kischinovsky for help with the manuscript.

REFERENCES

- 1 Imberty, A., and Pérez, S. A revisit to the three-dimensional structure of B-type starch. *Biopolymers* 1988, **27**, 1205–1221
- 2 Pitera, J., and Kollman, P.A. Graphical visualization of mean hydration from molecular dynamics simulations. *J. Mol. Graphics Modelling* 1997, **15**, 355–358
- 3 Stillinger, F.H., and Rahman, A. Improved simulation of liquid water by molecular dynamics. *J. Chem. Phys.* 1974, **60**, 1545–1557
- 4 Brooks, C.L., Karplus, M., and Pettitt, B.M. *Proteins: A Theoretical Perspective of Dynamics, Structure and Thermodynamics*. Wiley-Interscience, New York, 1988
- 5 Brady, J.W. Molecular dynamics simulations of α -D-glucose in aqueous solution. *J. Am. Chem. Soc.* 1989, **111**, 5155–5165
- 6 van Eijck, B.P., and Kroon, J. Molecular-dynamics simulations of β -D-ribose and β -D-deoxyribose solutions. *J. Mol. Struct.* 1989, **195**, 133–146
- 7 Engelsens, S.B., and Pérez, S. The hydration of sucrose. *Carbohydr. Res.* 1996, **292**, 21–38
- 8 Rossky, P.J., and Karplus, M. Solvation. A molecular dynamics study of a dipeptide in water. *J. Am. Chem. Soc.* 1979, **101**, 1913–1937
- 9 Brady, J.W., and Liu, Q. Anisotropic solvent structuring in aqueous sugar solutions. *J. Am. Chem. Soc.* 1996, **118**, 12276–12286
- 10 Immel, S., and Lichtenthaler, F.W. The conformation of sucrose in water: a molecular dynamics approach. *Liebigs Annalen* 1995, 1925–1937
- 11 Brooks, B.R., Brucoleri, R.E., Olafson, B.D., States, D.J., Swaminathan, S., and Karplus, M. CHARMm: A program for macromolecular energy, minimization and dynamics calculations. *J. Comput. Chem.* 1983, **4**, 187–217
- 12 Ha, S.N., Giammona, A., Field, M., and Brady, J.W. A revised potential-energy surface for molecular mechanics of carbohydrates. *J. Comput. Chem.* 1988, **180**, 207–221
- 13 Jorgensen, W.L. Transferable intermolecular potential functions for water, alcohols, and ethers. Application to liquid water. *J. Am. Chem. Soc.* 1981, **103**, 335–340
- 14 Engelsens, S.B., Hervé du Penhoat, C., and Pérez, S. Molecular relaxation of sucrose in aqueous solution: how a nanosecond molecular dynamics simulation helps to reconcile NMR data. *J. Phys. Chem.* 1995, **99**, 13334–13351
- 15 Engelsens, S.B., and Pérez, S. Internal motions and hydration of sucrose in a diluted water solution. *J. Mol. Graphics Modelling* 1997, **15**, 122–131
- 16 Galema, S.A., and Høiland, H. Stereochemical aspects of hydration of carbohydrates in aqueous solutions. 3. Density and ultrasound measurements. *J. Phys. Chem.* 1991, **95**, 5321–5326
- 17 Casset, F., Hamelryck, T., Loris, R., Brisson, J.R., Teller, C., Dao-Thi, M.-H., Wyns, L., Portemans, F., Pérez, S., and Imberty, A. NMR, molecular modeling, and crystallographic studies of lentil lectin–sucrose interaction. *J. Biol. Chem.* 1995, **270**, 25619–25628
- 18 Pérez, S., Imberty, A., Engelsens, S.B., Gruza, J., Mazeau, K., Jiménez-Barbero, J., Poveda, A., Espinoza, J.F., van Eijck, B.P., Johnson, G., French, A.D., Kouwijzer, M.L.C.E., Grootenhuis, P.D.J., Bernardi, A., Raimondi, L., Senderowitz, H., Durier, V., Vergoten, G., and Rasmussen, K. A comparison and chemometric analysis of several molecular mechanics force fields and parameters sets applied to carbohydrates. *Carbohydr. Res.* 1999